Light-Induced Insertion of a CO Ligand into an Os−N Bond of the Clusters $Os_3(CO)_{10}(L)$, Where L Represents a Potentially Terdentate *N,N′*-Chelating α-Diimine

Jos Nijhoff, František Hartl,*,† and Derk J. Stufkens

Anorganisch Chemisch Laboratorium, Institute of Molecular Chemistry, Universiteit van Amsterdam, Nieuwe Achtergracht 166, 1018 WV Amsterdam, The Netherlands

Jan Fraanje

Laboratorium voor Kristallografie, Institute of Molecular Chemistry, Universiteit van Amsterdam, Nieuwe Achtergracht 166, 1018 WV Amsterdam, The Netherlands

Received May 17, 1999

Irradiation of the clusters $Os_3(CO)_{10}(L)$ (L = pyridine-2-carbaldehyde-*N′*-R imine (R−PyCa), R = $Me_2N(CH_2)_2$ (**1**), $Me_2N(CH_2)_3$ (**5**), (2-pyridyl)$(CH_2)_2$ (**3**); L = 2-acetylpyridine-*N′*-R imine (R−AcPy), R = $Me_2N(CH_2)_2$ (**2**), (2-pyridyl)$(CH_2)_2$ (**4**)) with visible light leads to the formation of the novel CO-bridged ($Os^1C(O)N'Os^3$; N′ = imine nitrogen) photoproducts $Os_3(CO)_9(\mu\text{-}1\kappa C^{(CO)}\text{:}1\kappa C^{(imine)}\text{:}3\kappa^3 N,N',N''(R)\text{-L-}N'\text{-C(O)})$ (2 *Os−Os*), **1b**−**5b**, demonstrating the profound influence of the pendant Lewis base on the course of the photoreactions. Formation of the products **1b**−**5b** occurs via the initial formation of a zwitterion. The efficiency of this step determines the quantum yield of the photoreaction. In strongly coordinating solvents (e.g., S = pyridine, acetonitrile) this is the solvent-stabilized zwitterion $(CO)_4Os^-Os(CO)_4Os^+(CO)_2(S)(\kappa^2 N,N'\text{-L})$, whereas in noncoordinating solvents and in THF at ambient temperatures this is the intramolecularly stabilized zwitterion $(CO)_4Os^-Os(CO)_4Os^+(CO)_2(\kappa^3 N,N',N''(R)\text{-L})$. The latter species is formed from the corresponding biradical (the primary photoproduct in these solvents) via attack of the pendant Lewis base on the $\{Os^+(CO)_2(\kappa^2 N,N'\text{-L}^{\bullet-})\}$ moiety, inducing an electron-transfer reaction. The biradical also undergoes a radical coupling side reaction, affording an unstable η^2-imine-bridged product with the coordinatively unsaturated $Os(CO)_2(L)$ moiety, similar to an intermediate previously observed in the photoisomerization of $Os_3(CO)_{10}$(R−PyCa) (R = alkyl). This path does not contribute significantly to the net product formation. The novel compounds **1b**−**5b** have been characterized by IR and (with the exception of thermally unstable **4b**) NMR spectroscopy. The structure of **2b** has been determined by an X-ray diffraction study.

Introduction

Light-induced homolysis of metal−metal bonds has been reported for many binuclear complexes containing α-diimine ligands.[1] The reactions produce radicals that regenerate the parent complexes, dimerize, or undergo radical coupling reactions with formation of novel compounds.[2,3] In addition they may undergo an electron-transfer reaction with formation of ionic products.[4,5] For instance, the radicals $[Mn(CO)_3(\alpha\text{-diimine})]^\bullet$ and $^\bullet Mn(CO)_5$ formed on irradiation of $[Mn_2(CO)_8(\alpha\text{-diimine})]$ produce the ions $[Mn(CO)_5]^-$ and $[Mn(L_b)(CO)_3(\alpha\text{-diimine})]^+$ in the presence of a Lewis base (L_b).[6] Either these ions are stable in solution or they regenerate the starting complexes. Similarly, we have recently reported that the trinuclear clusters $Os_3(CO)_{10}(\alpha\text{-diimine})$ may produce either biradicals or zwitterions on irradiation with visible light, depending on the α-diimine ligand, coordinating ability of the added Lewis bases (e.g., donor solvent, PR_3 or halide), and the temperature.[7] Examples of the α-diimine ligands used are 2,2′-bipyrimidine, R−AcPy, and R−PyCa.[8] Solvent-stabilized zwitterions $(CO)_4Os^-Os(CO)_4Os^+(S)(CO)_2(\alpha\text{-diimine})$, produced in strongly coordinating acetonitrile and pyridine (= S),[7,9] are long-lived (seconds to minutes) and revert thermally to their parent cluster. Pressure-dependent quantum yield studies suggest that in these solvents the zwitterions are formed directly from the reactive excited state[10] via a concerted mech-

† E-mail: hartl@anorg.chem.uva.nl. Fax: +31-20-525 6456.

(1) Stufkens, D. J.; Aarnts, M. P.; Nijhoff, J.; Rossenaar, B. D.; Vlček Jr., A. *Coord. Chem. Rev.* **1998**, *171*, 93, and references therein.

(2) van der Graaf, T.; Stufkens, D. J.; Oskam, A.; Goubitz, K. *Inorg. Chem.* **1991**, *30*, 599.

(3) Nieuwenhuis, H. A.; van Loon, A.; Moraal, M. A.; Stufkens, D. J.; Oskam, A.; Goubitz, K. *J. Organomet. Chem.* **1995**, *492*, 165.

(4) Kokkes, M. W.; de Lange, W. G. J.; Stufkens, D. J.; Oskam, A. *J. Organomet. Chem.* **1985**, *294*, 59.

(5) van Dijk, H. K.; van der Haar, J.; Stufkens, D. J.; Oskam, A. *Inorg. Chem.* **1989**, *28*, 75.

(6) van der Graaf, T.; Hofstra, R. M. J.; Schilder, P. G. M.; Rijkhoff, M.; Stufkens, D. J.; van der Linden, J. G. M. *Organometallics* **1991**, *10*, 3668.

(7) Nijhoff, J.; Bakker, M. J.; Hartl, F.; Stufkens, D. J.; Fu, W.-F.; van Eldik, R. *Inorg. Chem.* **1998**, *37*, 661.

(8) Ligand nomenclature: R−AcPy = 2-acetylpyridine−*N′*−R imine, R−PyCa = pyridine-2-carbaldehyde−*N′*−R imine, and R−DAB = *N,N′*-di-R-1,4-diaza-1,3-butadiene in which R = alkyl group.

(9) van Outersterp, J. W. M.; Garriga Oostenbrink, M. T.; Nieuwenhuis, H. A.; Stufkens, D. J.; Hartl, F. *Inorg. Chem.* **1995**, *34*, 6312.

10.1021/om990366o CCC: $18.00
Publication on Web 09/23/1999

anism.[7] In the weaker coordinating solvent THF and in noncoordinating solvents, biradicals $(CO)_4Os^{\bullet}Os(CO)_4Os^{+}(CO)_2(\alpha\text{-diimine}^{\bullet-})$ are produced at room temperature.[7] These biradicals are short-lived (10−1000 ns) and also revert to the parent clusters $Os_3(CO)_{10}(\alpha\text{-diimine})$. In some cases, when α-diimine ligands with reactive imine bonds (e.g., R−DAB[8]) are employed, the biradicals and zwitterions may react further to give secondary products such as η^2-imine-bridged isomers.[11]

Eventhough the dipolar nature of the triosmium zwitterions has been deduced from ^{1}H NMR, UV−vis, and resonance Raman data,[7,9] their dipole moment has only recently been determined directly with the aid of time-resolved microwave conductivity (TRMC). This technique makes it possible to establish the photochemical formation of a solute dipole and/or to follow its decay as a function of time by measuring the change in conductivity of the solution caused by the dipole formation. TRMC has often been applied to characterize the charge-separated D^+A^- states of organic donor−acceptor systems[12−18] but not to study dipolar organometallic species. Unfortunately, the utilization of this technique is restricted to nonpolar solvents, i.e., cyclohexane, benzene, or 1,4-dioxane. Therefore, TRMC is not applicable for the study of the triosmium zwitterions stabilized in coordinating solvents, as these solvents have large dipole moments.

The efficient conversion of biradicals into zwitterions in a nonpolar solvent requires addition of a large excess of a Lewis base (e.g., acetonitrile), as the biradicals are typically short-lived (10^{-9}−10^{-8} s). The presence of such a high concentration of dipoles prevents the observation of the small change in permittivity caused by the change of dipole moment of the solute. An alternative way of converting the biradicals formed in an apolar solvent into zwitterions is to incorporate a Lewis base directly into the α-diimine ligand. This may be achieved by using, instead of an ordinary bidentate ligand as in our previous studies,[7,9,11] a potentially terdentate derivative, having a third N-donor group as a pendant sidearm. This pendant Lewis base may then convert the biradical into a zwitterion by attacking the open coordination site

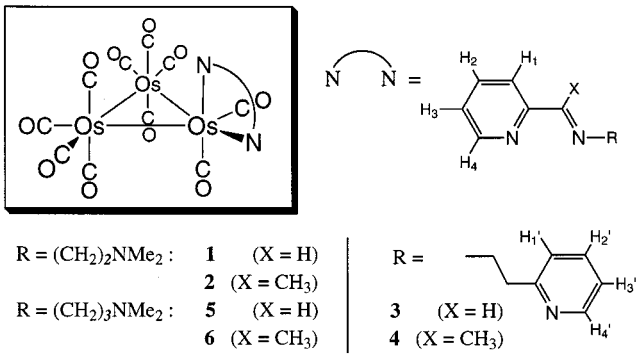

Figure 1. Schematic structure of the triosmium clusters **1**−**6** and the stuctures and adopted atom numbering of the R−PyCa (X = H) and R−AcPy (X = CH_3) ligands.

at the $\{Os^{+}(CO)_2(\alpha\text{-diimine}^{\bullet-})\}$ part of the biradical. The sidearm then has the same function as the acetonitrile molecules, while the permittivity of the solution remains unaffected.

To find out if such internally stabilized triosmium zwitterions can be produced, a series of triosmium clusters containing a potentially terdentate R−PyCa or R−AcPy ligand[8] has been prepared (**1**−**6**). Their structures are schematically depicted in Figure 1. The sidearm consists of a pendant Me_2N− or 2-pyridyl group, linked via either two or three methylene groups to the coordinating imine N atom of the α-diimine ligand. Recently, we have shown that the cluster $Os_3(CO)_{10}(Me_2N(CH_2)_3AcPy)$ (**6**) indeed transforms on visible irradiation into a long-lived (seconds) zwitterion even in noncoordinating solvents.[19] The dipole moment of the internally stabilized zwitterion (13 ± 2 D) could be determined for the first time from the TRMC signal in cyclohexane and benzene. In this paper, we have focused on the photoreactions of the other clusters in the series (**1**−**5**) that instead convert into a novel photoproduct. We here present the structure of this photoproduct and demonstrate that the reaction mechanism involves the same intramolecularly coordinated zwitterions as for **6**, which are, however, highly reactive in the case of **1**−**5**.

Experimental Section

Materials and Preparations. $Os_3CO)_{12}$ (ABCR), 2-pyridinecarboxaldehyde, 2-acetylpyridine and 3-(dimethylamino)-propylamine (Acros), 2-(2-aminoethyl)pyridine, and *N*,*N*-dimethylethylenediamine (Aldrich) were used as purchased. Trimethylamine-*N*-oxide dihydrate, $Me_3NO{\cdot}2H_2O$ (Alfa), was dehydrated before use by vacuum sublimation. Solvents of analytical (acetonitrile, 2-chlorobutane, pyridine, and THF) or spectroscopic grade (toluene) quality were dried over sodium wire (THF, toluene), CaH_2 (acetonitrile, pyridine), or anhydrous $CaCl_2$ (2-chlorobutane) and freshly distilled under nitrogen. Pyridine, 2-chlorobutane, and acetonitrile were stored on molecular sieves. The ligands R−PyCa[8,20,21] and R−AcPy[8,22] were prepared according to published procedures, using the appropriate amines.

(10) The UV−vis spectra of $Os_3(CO)_{10}(\alpha\text{-diimine})$ exhibit several close-lying absorption bands in the visible region (typically between 400 and 600 nm). The corresponding electronic transitions have recently been shown by DFT calculations (ref 37) to posess, due to the low symmetry of the clusters, a mixed $d\pi$(Os)-to-π^*(α-diimine) (MLCT) and $\sigma(Os_3)$-to-π^*(α-diimine) ($\sigma\pi^*$) character. The low-energy excited states are therefore denoted as MLCT/$\sigma\pi^*$. Their population significantly weakens the bonding within the triosmium core and results in cleavage of an $(\alpha\text{-diimine})(CO)_2Os{-}Os(CO)_4$ bond.

(11) Nijhoff, J.; Bakker, M. J.; Stufkens, D. J.; Hartl, F. *J. Organomet. Chem.* **1999**, *572*, 271−281.
(12) Mes, G. F.; de Jong, B.; van Ramesdonk, H. J.; Verhoeven, J. W.; Warman, J. M.; de Haas, M. P.; Horsman-van den Dool, L. E. W. *J. Am. Chem. Soc.* **1984**, *106*, 6524.
(13) Warman, J. M.; de Haas, M. P.; Oevering, H.; Verhoeven, J. W.; Paddon-Row, M. N.; Oliver, A. M. *Chem. Phys. Lett.* **1986**, *128*, 95.
(14) Lawson, J. M.; Paddon-Row: M. N.; Schuddeboom, W.; Warman, J. M.; A. H. A., C.; Ghiggino, K. P. *J. Phys. Chem.* **1993**, *97*, 13099.
(15) Roest, M. R.; Verhoeven, J. W.; Schuddeboom, W.; Warman, J. M.; Lawson, J. M.; Paddon-Row, M. N. *J. Am. Chem. Soc.* **1996**, *118*, 1762.
(16) Brouwer, A. M.; Eijckelhoff, C.; Willemse, R. J.; Verhoeven, J. W.; Schuddeboom, W.; Warman, J. M. *J. Am. Chem. Soc.* **1993**, *115*, 2988.
(17) van Dijk, S. I.; Wiering, P. G.; Groen, C. P.; Brouwer, A. M.; Verhoeven, J. W.; Schuddeboom, W.; Warman, J. M. *J. Chem. Soc., Faraday Trans.* **1995**, *91*, 2107.
(18) Warman, J. M.; Abellon, R. D.; Verhey, H. J.; Verhoeven, J. W.; Hofstraat, J. W. *J. Phys. Chem. B* **1997**, *101*, 4913.
(19) Nijhoff, J.; Hartl, F.; Stufkens, D. J.; Piet, J. J.; Warman, J. M. *J. Chem. Soc., Chem. Commun.* **1999**, 991.
(20) Brunner, H.; Riepl, G.; Benn, R.; Rufinska, A. *J. Organomet. Chem.* **1983**, *253*, 93.
(21) Brunner, H.; Reiter, B.; Riepl, G. *Chem. Ber.* **1984**, *117*, 1330.
(22) Lavery, A.; Nelson, S. M. *J. Chem. Soc., Dalton Trans.* **1985**, 1053.

The clusters **1**−**6** were synthesized using a procedure described previously.[7] All complexes were characterized by IR (ν(CO) in cm^{-1}; in 2-chlorobutane), ^1H NMR (δ in ppm; in $CDCl_3$; for numbering see Figure 1), UV-vis (λ_{max} in nm (ϵ_{max} in M^{-1} cm^{-1}); in THF), and mass (M^+ found (calculated)) spectroscopy. The spectral data testified the purity of **1**−**6** and their close similarity to the previously described $Os_3(CO)_{10}$(α-diimine) clusters.[7,9] For this reason **1**−**6** were not subjected to elemental analyses.

$Os_3(CO)_{10}(Me_2N(CH_2)_2PyCa)$ (**1**): IR 2086 m, 2037 s, 2008 s, 1995 s, 1980 s, 1964 m, 1961 sh, 1910 w; ^1H NMR 9.43 (d, 1H, H4), 8.85 (s, 1H, N=C−*H*), 8.01 (d, 1H, H1), 7.79 (dt, 1H, H2), 7.15 (dt, 1H, H3), 4.45 (m, 2H, =N−*CH*$_2$), 2.96 (m, 1H, C*H*$_2$NMe$_2$), 2.90 (m, 1H, C*H*$_2$NMe$_2$), 2.37 (s, 6H, N*Me*$_2$); UV−vis 563 (7610); MS 1028 (1027.97).

$Os_3(CO)_{10}(Me_2N(CH_2)_2AcPy)$ (**2**): IR 2085 m, 2036 s, 2007 s, 1993 s, 1978 s, 1962 m, 1958 sh, 1907 w; ^1H NMR 9.52 (d, 1H, H4), 7.99 (d, 1H, H1), 7.85 (dt, 1H, H2), 7.21 (dt, 1H, H3), 4.57 (m, 1H, =N−C*H*$_2$), 4.38 (m, 1H, =N−C*H*$_2$), 2.82 (m, 2H, *CH*$_2$NMe$_2$), 2.62 (s, 3H, N=C−*CH*$_3$), 2.32 (s, 6H, N*Me*$_2$); UV−vis 549 (5300); MS 1043 (1042.00).[11]

$Os_3(CO)_{10}$((2-pyridyl)$(CH_2)_2$PyCa) (**3**): IR 2087 m, 2038 s, 2009 s, 1996 s, 1981 s, 1966 m, 1960 sh, 1910 w; ^1H NMR 9.41 (d, 1H, H4), 8.57 (d, 1H, H4′), 8.50 (s, 1H, N=C−*H*), 7.74 (m, 2H, H1+H2′), 7.52 (dt, 1H, H2), 7.12 (m, 2H, H3+H3′+H1′), 4.75 (m, 2H, =N−*CH*$_2$), 3.49 (m, 1H, C*H*$_2$−(2-pyridyl)), 3.33 (m, 1H, C*H*$_2$−(2-pyridyl)); UV−vis 565 (8038); MS 1062 (1061.98).

$Os_3(CO)_{10}$((2-pyridyl)$(CH_2)_2$AcPy) (**4**): IR 2086 m, 2036 s, 2008 s, 1994 s, 1979 s, 1964 m. 1958 sh, 1907 w; ^1H NMR 9.52 (d, 1H, H4), 8.56 (d, 1H, H4′), 7.99 (d, 1H, H1), 7.82 (dt, 1H, H2′), 7.56 (dt, 1H, H2), 7.19 (m, 3H, H3+H3′+H1′), 2.42 (s, 3H), 4.92 (m, 1H, =N−*CH*$_2$), 4.55 (m, 1H, =N−C*H*$_2$), 3.42 (m, 1H, C*H*$_2$−(2-pyridyl)), 3.22 (m, 1H, C*H*$_2$−(2-pyridyl)); UV−vis 551 (7663); MS 1077 (1076.01).

$Os_3(CO)_{10}(Me_2N(CH_2)_3PyCa)$ (**5**)**:** IR 2087 m, 2038 s, 2009 s, 1995 s, 1980 s, 1965 m, 1961 sh, 1911 w; ^1H NMR 9.44 (d, 1H, H4), 8.80 (s, 1H, N=C−*H*), 7.96 (d, 1H, H1), 7.79 (dt, 1, H2), 7.16 (dt, 1H, H3), 4.41 (m, 2H, =N−*CH*$_2$), 2.23 (m, 2H, *CH*$_2$NMe$_2$), 2.20 (s, 6H, N*Me*$_2$), 2.18 (m, 1H, =N−CH$_2$C*H*$_2$), 1.97 (m, 1H, =N−CH$_2$C*H*$_2$); UV−vis 564 (6040); MS 1043 (1042.00).

$Os_3(CO)_{10}(Me_2N(CH_2)_3AcPy)$ (**6**): IR (toluene) 2086 m, 2036 s, 2009 s, 1991 s, 1977 s, 1963 m, 1956 m, 1906 w; ^1H NMR (223 K, THF-d_8) 9.54 (d, 1H, H4), 8.45 (d, 1H, H1), 8.13 (dd, 1H, H2), 7.48 (dd, 1H, H3), 4.73 (m, 1H, =N−C*H*$_2$), 4.16 (m, 1H, =N−C*H*$_2$), 2.80 (s, =C−C*H*$_3$), 2.19 (s, 6H, N(C*H*$_3$)$_2$); UV−vis 549 (5270); MS 1058 (1056.99).

Spectroscopic Measurements. UV−vis spectra were recorded on a Varian Cary 4E spectrophotometer, and FTIR spectra on a Bio-Rad FTS-7 or FTS-60A spectrometer. An Oxford Instruments DN 1704/54 liquid-nitrogen cryostat was used for low-temperature spectroscopic measurements. ^1H NMR spectra were obtained with a Bruker AMX 300 spectrometer. Field desorption mass spectra were collected on a JEOL JMS SX/SX102A four-sector mass spectrometer coupled to a JEOL-MP 7000 data system.

Continuous-Wave Photochemistry. A Spectra Physics 2025 argon-ion laser was generally used for the photochemical experiments. The light-sensitive samples (10^{-3}−10^{-4} M) were prepared in a carefully blinded room, illuminated with red light. To record the ^1H NMR spectra of the photoproducts, a solution of the parent cluster in $CDCl_3$ was irradiated with λ > 420 nm (using a water-cooled Oriel AG 150 mW high-pressure Xe lamp equipped with a cutoff filter) at ca. 253 K within a CIDNP probe or at 298 K in dichloromethane with the 514.5 nm line of an argon-ion laser in a homemade large-volume thin-layer cell[23] outside the NMR spectrometer cavity.

(23) Nijhoff, J. Ph.D. Thesis, University of Amsterdam, Amsterdam, The Netherlands, 1998; p 24.

Table 1. Crystallographic Data for Photoproduct 2b

formula	$C_{21}H_{17}N_3O_{10}Os_3$
molecular weight	1042.0
crystal dimens (mm)	0.10 × 0.25 × 0.25
space group	$P2_1/c$
a, *b*, *c* (Å)	11.1308(7), 15.311(1), 15.404(2)
β (deg),	100.000(8)
V (Å^3)	2585.3(4)
Z	4
ρ_{calc} (g cm^{-3})	2.68
λ (Cu Kα , Å),	1.5418
abs coeff (cm^{-1})	277.4
scan technique	$\omega-2\theta$
F(000), *T* (K)	1888, 223
no. of unique reflns	5295
h, *k*, *l* range	$-13 \le h \le 13$, $0 \le k \le 19$, $0 \le l \le 19$
no. of obsd reflns	4714
data rejected if *I*	$<2.5\sigma(I)$
$((\sin\theta)/\lambda)_{max}$	0.63 Å^{-1}
weighting scheme	$[50.0 + 10^{-3}(\sigma(F_{obs}))^2 + 10^{-4}/(\sigma(F_{obs}))]^{-1}$
final *R*, R_w	0.090, 0.103
$(\Delta/\sigma)_{max}$, *S*	0.44, 1.73(2)

In the latter case, the solvent was evaporated after the irradiation interval and the product was redissolved in $CDCl_3$. Quantum yields of the disappearance of the parent clusters were determined by UV−vis spectroscopy, following an automated procedure. The sample solution was kept in a thermostated 1 cm cuvette and irradiated via an optical fiber inside the sample compartment of the spectrophotometer. The solution was well stirred during the irradiation intervals, and the conversion per interval was kept below 5%. Light intensities were measured with a Coherent 212 powermeter calibrated with an Aberchrome 540 solution according to literature procedures.[24,25] In the computational routine[26] corrections were made for changes in the partial absorption of the photoactive species caused by both its depletion and by the inner filter effect of the photoproduct(s) formed.[27]

For the photoconversion of cluster **5** into **5b** in toluene the pressure dependence of the quantum yield Φ_5 was studied with a setup described previously.[28] Samples were irradiated under four different pressures between 0.1 and 150 MPa in a pillbox quartz cell[29] placed inside a two-window high-pressure cell.[30] The solutions were stirred by a Teflon-coated magnetic stirrer during irradiation with the light (λ = 508 nm) of an Oriel 100 W high-pressure mercury lamp. Light intensities were measured by a Si photodiode calibrated at 508 nm with Actinochrome N. The incident light intensity was kept in the range (1.3−1.4) × 10^{-9} einstein s^{-1}.

Crystal Structure Determination of the Photoproduct 2b. Colorless crystals of **2b** were obtained by slow evaporation of a dichloromethane solution of **2** left in daylight. Crystallographic data were recorded on an Enraf-Nonius CAD-4 diffractometer and are summarized in Table 1.

Two reference reflections ($\bar{1}$ 3 3), (1 1 0) were measured hourly and showed a 10% decrease over the 70 h collection time, which was corrected for. Unit-cell parameters were refined by a least-squares fitting procedure using 23 reflections with 80° < 2θ < 84° and corrected for Lorentz and polarization effects. Absorption correction was performed with the program

(24) Heller, H. G.; Langan, J. R. *J. Chem. Soc., Perkin Trans. 2* **1981**, 341.
(25) Aberchromics Ltd., S.o.C.a.A.C., College of Cardiff, University of Wales.
(26) Kleverlaan, C. J. *Yield Methode II*; University of Amsterdam, 1992.
(27) Vichova, J.; Hartl, F.; Vlček, A., Jr. *J. Am. Chem. Soc.* **1992**, *114*, 10903.
(28) Wieland, S.; van Eldik, R.; Crane, D. R.; Ford, P. C. *Inorg. Chem.* **1989**, *28*, 3663.
(29) le Noble, W. J.; Schlott, R. *Rev. Sci. Instrum.* **1976**, *47*, 770.
(30) Fleischmann, F. K.; Conze, E. G.; Stranks, D. R.; Kelm, H. *Rev. Sci. Instrum.* **1974**, *45*, 1427.

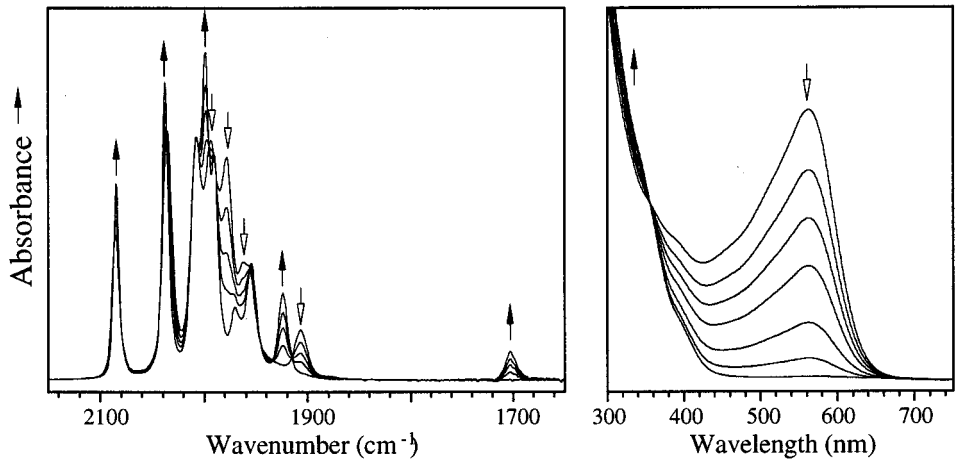

Figure 2. Infrared (left) and UV−vis (right) spectral changes accompanying the formation of the photoproduct **2b** by irradiation of **2** in 2-chlorobutane at 298 K.

ABSCAL[31] using ψ-scans of the [2 0 6] reflection, with coefficients in the range 1.0−5.51. The structure was solved by direct methods. The positions of the hydrogen atoms were calculated. Full-matrix least-squares refinement was performed on *F*, anisotropic for the non-hydrogen atoms and isotropic for the hydrogen atoms, keeping their temperature factors fixed at $U = 0.125$ Å^2, restraining the hydrogens in such a way that the distance to their carrier remained constant at approximately 1. The secondary isotropic extinction coefficient[32,33] refined to Ext = 0.05(4). A final difference Fourier map revealed a residual electron density between −11.25 and 5.84 e Å^{-3}. Scattering factors were taken from the literature.[34,35] All calculations were performed with XTAL,[36] unless stated otherwise.

Results

All the clusters **1**−**5** possess very similar IR CO-stretching band patterns (see Experimental Section). Their UV−vis spectra exhibit a strong absorption band at 550−600 nm, which belongs to an electronic transition of prevailing MLCT character within the $Os(CO)_2$-(α-diimine) moiety.[7,9,10,37] In addition, there are several bands between 400 and 550 nm, which may well be associated with $\sigma\pi^*$ transitions.[10] The IR and UV−vis spectral properties are hardly influenced by variation of the pendant N-donor substituent. The photoreactions of **1**−**5** were studied by irradiation into the visible absorption band both at room and low temperatures, in coordinating as well as noncoordinating solvents. The photoreactions were monitored by IR and UV−vis spectroscopy and were mainly performed in 2-chlorobutane since this solvent is virtually transparent in the 2200−1600 cm^{-1} region. This latter property was particularly important for the unambiguous identification of weak IR bands belonging to bridging carbonyl ligands.

Photolysis in Noncoordinating Solvents. Irradiation of solutions of the clusters **1**−**5** in hexane, toluene, 2-chlorobutane, dichloromethane, or THF at room temperature led to the formation of a novel type of photoproduct, to be called hereafter **1b**−**5b**, which had not been observed in previous studies.[7,9,11,19] Except for **4b**, solutions of **1b**−**5b** are thermally stable at room temperature for several hours. In THF and 2-chlorobutane, **4b** decomposes within a few minutes into unidentified products; in toluene it regenerates **4** within ca. 10 min with only little decomposition.

The changes in the IR and UV−vis spectra accompanying the conversion of **2** into **2b** are presented in Figure 2. The IR data of the products **1b**−**5b** are collected in Table 2. Formation of the new product is accompanied by the disappearance of the MLCT band (around 560−580 nm). This effect implies that the π-conjugation of the α-diimine ligand has been lifted in **1b**−**5b**. The CO-stretching vibrations are still found in the same frequency region as they are for the parent cluster, although changes in relative intensities, small frequency shifts, and sharpening of several bands occur. This implies that the photoproduct is still a largely intact triosmium cluster. There is however one remarkable change with respect to the IR spectrum of the parent cluster. A weak, but distinct new band appears at 1700 cm^{-1}, which clearly belongs to a bridging CO group. The origin of this band will become clear from the X-ray structure of **2b**, presented in the following section.

The ^{1}H NMR data of the photoproducts are collected in Table 3 (see Figure 1 for numbering scheme). Due to its thermal instability at room temperature, no NMR data could be obtained for **4b**. Although the photoproducts contain different substituents R at the R−PyCa and R−AcPy ligands, their ^{1}H NMR spectra show several similarities. The resonance of the *ortho*-proton H4 of the pyridine group has shifted by ca. 0.9 to a lower ppm value relative to that in **1**−**3** and **5**, just as that of H1. A small shift to lower ppm is also observed for the other pyridine protons H2 and H3. Most remarkable, however, is the resonance of the imine proton of the R−PyCa clusters, which shifts from above 8.5 ppm for **1**, **3**, and **5** to ca. 5.3 ppm in the case of **1b**, **3b**, and **5b**. The proton resonances of the pendant sidearm R of the ligands change significantly on formation of the photoproduct.

(31) Watenpaugh, K.; Stewart, J. M. *Physical and Analytical Chemistry*; The Upjohn Company, Kalamazoo, MI 49001, 1992.
(32) Zachariasen, W. H. *Acta Crystallogr.* **1967**, *A23*, 558.
(33) Larson, A. C. In *The Inclusion of Secondary Extinction in Least-Squares Refinement of Crystal Structures*; Ahmed, F. R., Hall, S. R., Huber, C. P., Eds.; Munksgaard: Copenhagen, 1970; pp 291−294.
(34) Cromer, D. T.; Mann, J. B. *Acta Crystallogr.* **1968**, *A24*, 321.
(35) Cromer, D. T.; Mann, J. B. *International Tables for X-ray Crystallography*; Kynoch Press: Birmingham, U.K., 1974; Vol. 4, p 55.
(36) Hall, S. R.; Stewart, J. M. *XTAL 3.2 Users Manual*; Universities of Western Australia and Maryland: Perth, Australia, and College Park, MD, 1992.
(37) (a) Calhorda, M. J.; Hunstock, E.; Veiros, L. F.; Hartl, F. *Organometallics*, submitted for publication. (b) Bakker, M. J.; Hartl, F.; Snoeck, T. L.; Calhorda, M. J.; Hunstock, E. Manuscript in progress.

Table 2. IR Data (ν(CO) in cm^{-1}) of the Photoproducts 1b−5b[a] and of the Zwitterions 2a′ and 4a′ [b] and 1a.S−5a.S[c]

1b	2086 m	2040 s	2006 sh	2000 vs	1990 s	1973 m	1957 m	1924 m	1706 w
2b	2085 s	2038 vs	2007 s	1999 vs	1990 s	1970 w	1955 m	1924 m	1703 w
3b	2084 m	2039 vs	2005 sh	2001 vs	1992 s	1972 w	1956 m	1928 w	1711 vw
4b	2084 m	2038 m	2004 sh	2000 vs	1991 s	1971 m	1954 m	1925 w	1700 vw
5b	2087 m	2040 s	2010 s	1999 vs	1992 s	1974 m	1957 m	1922 w	1708 vw
1a.S	2073 w	1995 vs	1968 s	1924 w	1895 w	1874 m			
2a.S	2072 w	1991 vs	1968 vs	1927 w	1897 w	1872 m			
3a.S	2074 w	1993 vs	1968 vs	1927 w	1898 w	1874 m			
4a.S	2072 w	1993 s	1968 vs	1931 w	1900 w	1873 m			
5a.S	2073 w	1995 vs	1969 s	1926 w	1899 w	1874 m			
2a′	2073 w	*d*	1972 s	*d*	1897 w	1874 m	1861 sh		
4a′	2075 w	1989 vs	1971 s	1922 w	1897 w	1872 m			
6a′ [e]	2073 w	1985 vs	1967 s	1921 w	1893 w	1870 m			

[a] 2-Chlorobutane, 298 K. [b] 2-Chlorobutane, 183 K. [c] Pyridine, 298 K. [d] Obscured by bands of **2b** formed together with **2a′** . [e] Reference 19.

Table 3. ^{1}H NMR Data of the Photoproducts 1b−3b and 5b in $CDCl_3$[d]

1b	8.53 (d, 1H, H4), 7.56 (dt, 1H, H2), 7.09 (d, 1H, H1), 6.99 (dt, 1H, H3), 5.21 (s, 1H, N=C−H), 3.80 (m, 1H, =N−CH_2), 3.26 (s, 3H, NMe_2), 2.63 (s, 3H, NMe_2), 2.58 (dd, 1H, =N−CH_2), 2.13 (s, 3H, NMe_2), 2.05 (m, 1H, CH_2NMe_2)[b]
2b	8.57 (d, 1H, H4), 7.65 (dt, 1H, H2), 7.07 (d, 1H, H1), 7.02 (dt, 1H, H3), 2.57 (s, 3H, N=C−CH_3), 3.64 (dt, 1H, =N−CH_2), 3.26 (s, 3H, NMe_2), 3.21 (dd, 1H, =N−CH_2), 2.63 (s, 3H, NMe_2), 2.13 (dd, 1H, CH_2NMe_2), 1.81 (dt, 1H, CH_2NMe_2)
3b	9.04 (d, 1H, H4′), 8.57 (s, 1H, H4), 7.78 (dt, 1H, H2′),7.55 (dt, 1H, H3′), 7.30 (m, 2H, H1′+H2), 7.00 (d, 1H, H1), 6.96 (t, 1H, H3), 5.28 (s, 1H, N=C−H), 3.47 (m, 2H, =N−CH_2), 3.22 (br m, 1H, CH_2−py), 2.97 (br m, 1H, CH_2−py)
5b	8.48 (d, 1H, H4), 7.51 (dt, 1H, H2), 7.00 (d, 1H, H1), 6.95 (dt, 1H, H2), 5.03 (s, 1H, N=C−H), 3.36 (t, 1H, =N−CH_2), 3.24 (s, 3H, NMe_2), 2.77 (t, 1H, =N−CH_2), 2.50 (m, 3H, =N−CH_2CH_2 (2H) + CH_2NMe_2 (1H)),[b] 2.13 (s, 3H, NMe_2)

[a] The ^{1}H NMR spectrum of thermally unstable **4b** could not be recorded. [b] Other resonance of the CH_2NMe_2 group obscured by solvent impurities. [c] The signal of H2 overlaps with that of H1′. [d] See Figure 1 for numbering scheme; py = 2-pyridyl.

Thus, the signals of the =N−CH_2 protons are generally more asymmetric and shift to lower ppm values. Moreover, the methyl groups of the terminal dimethylamino group of **1b**, **2b**, and **5b** become magnetically nonequivalent and show up as two singlets that are 0.7−0.9 ppm apart. These data indicate that the NMe_2 group, which is pendant in the parent clusters, becomes attached to a metal center in the photoproducts. In the case of **3b** the resonance of the *ortho*-proton H4′ shifts to 9.04 ppm, while the signals of H1′ and H3′ are split and shift to higher ppm values with respect to those of the parent cluster **3**. This again indicates that the pendant 2-pyridyl group becomes σ-bonded to an osmium center in **3b**.

Crystal Structure of the Photoproduct 2b. The spectral data in the preceding section indicate that the photoproducts **1b**−**5b** have a very similar structure in which one CO is bridging and the originally pendant NMe_2 or 2-pyridyl group has become coordinated to one of the osmium atoms. To determine this structure, an X-ray diffraction study was performed. The photoproducts **1b**, **3b**, and **5b** were not suited for this purpose, as they decomposed within a few days into a mixture of dark colored products, which were not further investigated. The product **2b** is however rather stable, and single crystals could be grown by slow evaporation of a dichloromethane solution at room temperature. Unfortunately, the crystals deteriorated considerably during the data collection, even at 223 K. As a result, the diffraction data are less accurate, and this is reflected in the rather high standard deviations and *R*-values.

Figure 3 presents a PLUTO drawing of the molecular structure of **2b**. A schematic representation can be found in Figure 4a. Selected bond distances and angles are collected in Table 4. Figure 3 shows that in **2b** all three

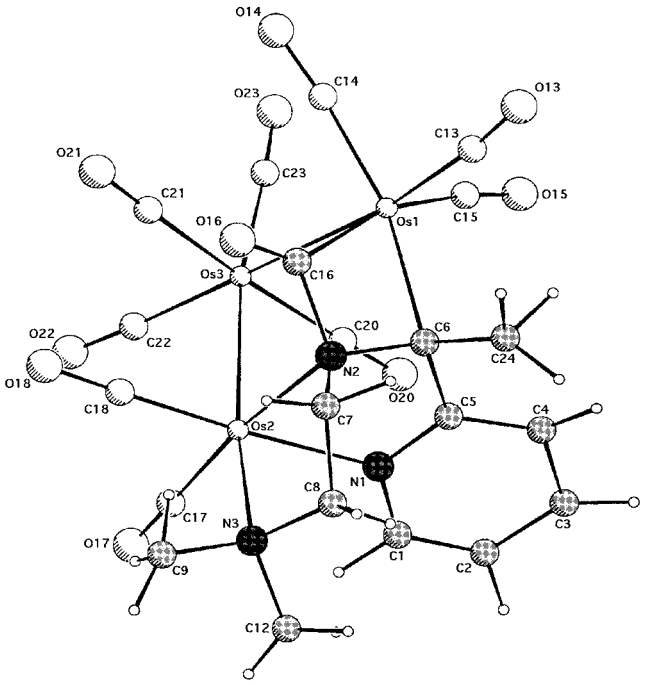

Figure 3. Pluto representation of the crystal structure of the photoproduct **2b**.

nitrogens of the $Me_2N(CH_2)_2AcPy$ ligand coordinate to the same osmium center (Os2). One Os−Os bond (Os1−Os2) is broken, and the imine carbon atom (C6) binds to the adjacent metal center (Os1). However, unlike in the isomeric products $Os_3(CO)_{10}(\kappa^2N,N',\mu_2$-N′,$\eta^2$-N′=C-α-diimine),[11,38] the imine nitrogen atom (N2) of **2b** is

(38) Zoet, R.; Jastrzebski, J. T. B. H.; van Koten, G.; Mahabiersing, T.; Vrieze, K.; Heijdenrijk, D.; Stam, C. H. *Organometallics* **1988**, *7*, 2108.

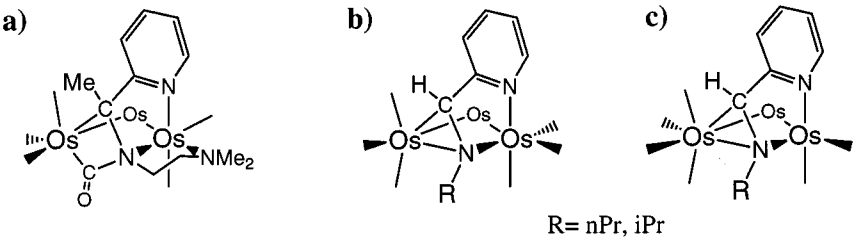

Figure 4. Schematic structures of (a) the photoproduct **2b** and (c) $Os_3(CO)_{10}(\kappa^2N,N',\mu_2\text{-}N',\eta^2\text{-}N'{=}C{-}R{-}PyCa)$ with the coordinatively unsaturated $Os(CO)_2(R{-}PyCa)$ site. The precursor of (b) the stable $(CO)_3Os{-}Os(CO)_4{-}Os(CO)_3(\kappa^2N,N',\mu_2\text{-}N',\eta^2\text{-}N'{=}C{-}R{-}PyCa)$ isomer in the case R = alkyl.[11] The four carbonyl groups at the Os atom in the rear are omitted for clarity.

Table 4. Selected Bond Distances (Å) and Angles (deg) for the Non-Hydrogen Atoms of 2b[a]

Os1−Os2	3.913(1)	C6−C24	1.51(4)	Os3−Os1−C16	82.2(6)	C20−Os3−C23	91(1)
Os1−Os3	2.925(1)	C1−N1	1.38(3)	Os3−Os2−N1	89.9(5)	C21−Os3−C22	90(1)
Os2−Os3	2.899(2)	C5−N1	1.38(3)	Os3−Os2−N2	90.1(5)	C6−N2−C16	99(2)
Os1−C6	2.22(2)	C1−C2	1.35(4)	Os2−N1−C16	108(1)	C7−N2−C16	114(2)
Os1−C16	2.10(3)	C2−C3	1.38(4)	N1−Os2−N3	87.3(8)	C17−Os2−N2	174(1)
$Os1{-}CO_{av}$	1.91(2)	C3−C4	1.40(4)	N2−Os2−N3	82.4(8)	C18−Os2−N1	176(1)
Os1−N2	2.73(2)	C4−C5	1.40(4)	C6−Os1−C14	161(1)	C1−C2−C3	119(2)
Os2−N1	2.11(2)	C5−C6	1.53(3)	C6−Os1−C15	103(1)	Os1−C6−N2	93(1)
Os2−N2	2.20(2)	C16−N2	1.51(3)	C6−Os1−C16	64.0(9)	C5−C6−N2	111(2)
Os2−N3	2.27(2)	C16−O16	1.19(3)	C14−Os1−C16	97(1)	Os1−C16−N2	98(1)
$Os2{-}CO_{av}$	1.87(4)	Os1−Os2−Os3	48.09(3)	C17−Os2−C18	87(1)	Os1−C16−O16	143(2)
$Os3{-}CO_{av}$	1.90(3)	Os1−Os3−Os2	84.41(4)	C20−Os3−C21	170(1)	C1−N1−C5	119(2)
C6−N2	1.50(3)	Os3−Os1−C6	94.8(6)	C20−Os3−C22	98(1)	Os2−N2−C6	110(1)

[a] Standard deviations are given in parentheses. The nonbonded distances Os1−Os2 and Os1−N2 are presented as well.

not bonded to Os1 but only to Os2. Instead, N2 and Os1 are connected by a bridging CO group, which is responsible for the new ν(CO) band in the IR spectrum of **2b** at 1700 cm^{-1} (vide supra). Further comments on this structure will be given in the Discussion.

Photolysis at Low Temperatures. The above experiments show that **1b**−**5b** are the only photoproducts and that no intramolecularly stabilized zwitterions are obtained in noncoordinating or weakly coordinating solvents at room temperature, as they are for cluster **6**. To investigate whether such zwitterions are formed as unstable intermediates, several low-temperature studies were performed. On irradiation of **1** and **3** in 2-chlorobutane at 183 K, identical IR and UV−vis spectral changes occurred due to the formation of **1b** and **3b**, as were observed at 298 K. For **2**, **4**, and **5**, however, additional ν(CO) bands arose at 183 K. Both **2** and also **4**, containing an R−AcPy ligand, formed a photoproduct not observed for the R−PyCa clusters **1**, **3**, and **5**. In the case of **2**, a moderately intense band was observed at 1874 cm^{-1}, with a shoulder at 1861 cm^{-1}. These two features are assigned to the internally stabilized zwitterion **2a′**.[39] For the cluster **4**, the zwitterion **4a′** was virtually the only product formed on irradiation in 2-chlorobutane at 183 K. The wavenumbers of the ν(CO) bands of **4a′** (2075 w, 2007 sh, 1996 sh, 1989 vs, 1971 s, 1922 m, 1897 w, and 1872 m cm^{-1}) nicely agree with those of the intramolecularly coordinated zwitterion **6a′** (2073 vw, 1985 vs, 1967 s, 1921 w, 1893 w, 1870 m, br)[19] as well as with those of the previously reported zwitterions.[7,9] When the solutions containing **2a′** and **4a′** were further irradiated or raised in temperature, **2b** and **4b**, respectively, were ultimately formed. Different from what was observed at 298 K, the product **4b** is thermally stable for hours at 233 K. In view of the fact that 2-chlorobutane can hardly coordinate, the zwitterions **2a′** and **4a′** must have been formed and stabilized by coordination of the pendant sidearm just as in the case of the intramolecularly stabilized zwitterion **6a′**.[19]

For cluster **5**, two additional weak ν(CO) bands are observed at 2115 and 2062 cm^{-1}, respectively, indicating the formation of a minor side product or intermediate **5′**. These wavenumbers are very close to those of the highest frequency ν(CO) bands previously reported for a cluster intermediate involved in the light-induced formation of the isomers $Os_3(CO)_{10}(\kappa^2N,N',\mu_2\text{-}N',\eta^2\text{-}N'{=}C{-}R{-}PyCa)$ (see Figure 4b) from $Os_3(CO)_{10}(\kappa^2N,N'\text{-}R{-}PyCa)$.[11] The structure of the cluster intermediate, depicted schematically in Figure 4c, and that of **5′** are therefore proposed to be very similar. The two detectable ν(CO) bands of **5′** disappear rapidly when the photoreaction is instead performed at a slightly higher temperature (T = 203 K). Irradiation of **2** in 2-chlorobutane at 183 K produces besides **2a′** and **2b** again the transient **2′** with detectable ν(CO) bands at 2121 and 2061 cm^{-1}. Just as **5′**, also **2′** is unstable and disappears when the irradiation at 183 K is stopped.

The formation of the intermediates **2′** and **5′**, the zwitterions **2a′** and **4a′**, and their conversion into the final products are depicted in Scheme 1.

Photolysis in Strongly Coordinating Solvents. The photochemical behavior of the clusters **1**−**5** in coordinating solvents such as acetonitrile or pyridine closely resembles that in noncoordinating solvents with respect to the final product formation (with the exception of **4**, vide infra). However, as might be expected in view of the behavior of the clusters with simple bidentate α-diimine ligands,[7] zwitterion formation is an important process in these solvents. Indeed, the primary photoproducts were exclusively the solvent-coordinated zwitterions **1a.S**−**5a.S**,[39] the IR data of which are

(39) The intramolecularly stabilized zwitterions are denoted as **na′**, the solvent-stabilized zwitterions as **na.S** (**n** = cluster number).

Scheme 1. Mutual Relation between the Photoproducts 1b−5b, the Intramolecularly (2a′, 4a′) and Solvent-Stabilized (1a.S−5a.S) Zwitterions, and the Low-Temperature Photoproducts 2′ and 5′[a]

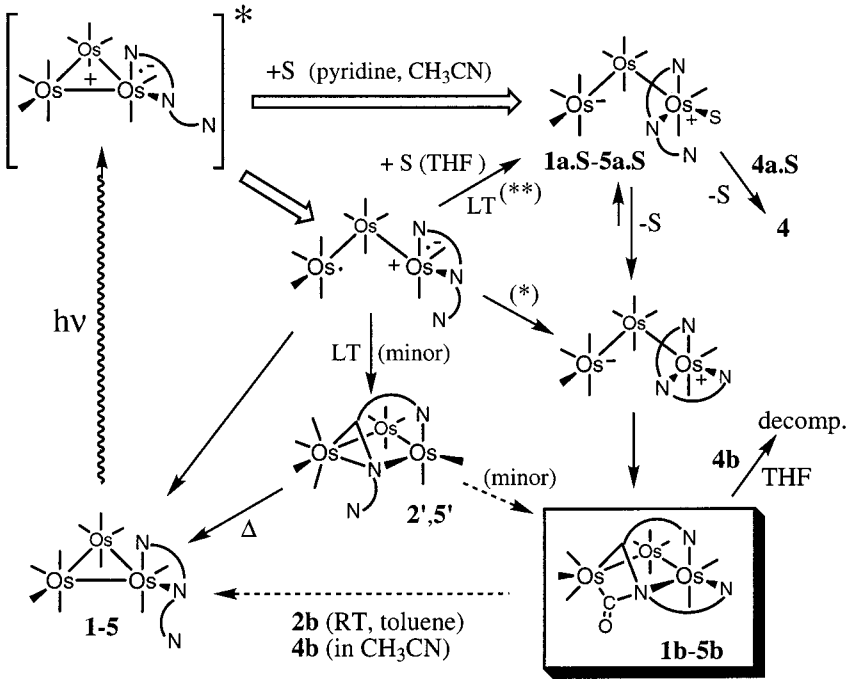

[a] (*) Only **2a′** and **4a′** are detectable at low temperatures. (**) Concluded from temperature-dependent quantum yield study of **5**.

presented in Table 2. However, contrary to the related zwitterions that contain R−PyCa and R−AcPy ligands without a pendant Lewis base and that are formed under the same conditions, **1a.S**−**3a.S** and **5a.S** are rather short-lived at room temperature. Their lifetimes vary from 3 s for **5a.S** to ca. 30 s for **2a.S** in pyridine and are even shorter in acetonitrile. The dependence of the lifetime on the solvent shows that we are dealing with solvent-stabilized zwitterions.

$Os_3(CO)_{10}(Me_2N(CH_2)_2AcPy)$ (**2**) and $Os_3(CO)_{10}$(2-pyridyl$(CH_2)_2$AcPy) (**4**), which have a methyl substituent at the imine carbon of their α-diimine ligand, differ again in the photoreaction course from the R−PyCa clusters **1**, **3**, and **5**. First of all, the zwitterions **2a.S** and **4a.S** are much longer lived than those derived from clusters **1**, **3**, and **5**. Even in acetonitrile, **2a.S** is sufficiently long-lived ($\tau = 5$ s) to be observed, whereas **1a.S**, **3a.S**, and **5a.S** could only be traced at room temperature by their transient ν(CO) band at ca. 1870 cm^{-1} or at lower temperatures ($T < 273$ K). The two R−AcPy clusters **2** and **4** differ also from **1**, **3**, and **5** in their ultimate product formation. The zwitterion **4a.S** does not produce any **4b** at all, but regenerates the parent cluster **4** within 7 min in pyridine and 340 s in acetonitrile. The zwitterion **2a.S** does transform into **2b**, but this product is not stable in acetonitrile (as it is in other solvents), slowly reconverting into the parent cluster **2**. After 12 min ca. 70% of the starting material is recovered in this way.

Quantum Yields. To study the influence of the imine substituents (different length of the sidearm; R−AcPy vs R−PyCa) on the efficiency of product formation, quantum yields for the disappearance of the parent clusters **1**, **2**, and **5** were determined in various solvents. In the case of the photoconversion of **5** into **5b**, the quantum yield Φ_5 was also measured in dependence on the irradiation wavelength, temperature, and applied pressure. The results are collected in Tables 5 and 6 and will be disacussed in the next section.

Table 5. Quantum Yields $\Phi \times 10^2$ (λ_{irr} in nm)[a] for the Disappearance of 1, 2, and 5 on Irradiation in Toluene, THF, and Acetonitrile

	toluene	THF			acetonitrile
cluster	Φ(514.5)	Φ(457.9)	Φ(488.0)	Φ(514.5)	Φ(514.5)
1	4.46	*b*	*b*	15.0	24.1
2	5.85	*b*	*b*	5.27	24.5
5	6.38	20.4	20.1	20.3	29.4

[a] $T = 298 \pm 0.2$ K; estimated relative error approximately 3%. [b] Wavelength dependence of Φ not determined.

Table 6. Quantum Yields $\Phi_5 \times 10^2$ for the Disappearance of 5 at Different Temperatures T[a] on Irradiation at 514.5 nm in Toluene and THF

	T (K)					
	248	258	268	278	288	298
toluene	3.80	4.25	4.69	5.22	5.68	6.38
THF	15.4	16.9	18.0	19.0	19.8	20.3

[a] $T \pm 0.2$ K; estimated relative error approximately 3% (except at 248 and 258 K: 5%).

The data in Table 5 show that the quantum yield Φ increases for all three clusters from 0.04−0.06 to 0.24−0.29 going from toluene to acetonitrile. The quantum yield Φ_5 does not depend on the wavelength of excitation but decreases on lowering the temperature. The temperature dependence of Φ_5 was determined in toluene as well as in THF in the temperature range 248−298 K (see Table 6). From corresponding Arrhenius plots, the apparent activation energies E_a and preexponential factors Φ_0 were derived. For the photoreaction in toluene a linear relation between ln(Φ_5) and $1/T$ is obtained, giving $E_a = 510 \pm 15$ cm^{-1} (~6.1 kJ/mol) and $\Phi_0 = 75$. In the case of THF, the Arrhenius plot is not

linear. At the highest temperatures used the slope of the curve corresponds to $E_a = 190 \pm 10$ cm^{-1} (~2.3 kJ/mol) and $\Phi_0 = 0.52$; at the lowest temperatures we find $E_a = 360 \pm 15$ cm^{-1} (~4.3 kJ/mol) and $\Phi_0 = 1.3$.

The pressure dependence of Φ_5 was studied in toluene. Increasing the pressure from 0.1 to 150 MPa resulted in a small decrease of Φ_5 from 0.0820 (0.1 MPa) to 0.0757 (50 MPa), to 0.0714 (100 MPa), and 0.0710 (150 MPa). From these data the apparent volume of activation $\Delta V^{\ddagger}$ is obtained from the slope of the linear plot of $\ln[\Phi/(1 - \Phi)]$ vs pressure.[28,40−47] Values derived from such plots are preferred over those obtained from $\ln \Phi$ vs pressure since they represent the difference between the volume of activation of the reaction and that of the nonradiative excited-state decay.[41] The resulting value of $\Delta V^{\ddagger} = +2.6 \pm 0.6$ cm^3 mol^{-1} is small, and mainly due to this fact the correlation coefficient is only 0.857.

Discussion

Structure of the Photoproducts 1b−5b. According to the spectral data collected in Tables 2 and 3, the products **1b**−**5b** differ from the zwitterions and the imine-bridged isomers described previously.[7,11] This is directly evident from the IR ν(CO) band patterns. Furthermore, the chemical shift of the imine proton, which is usually indicative of the imine coordination mode, is different for these products. For instance, the resonances of the imine protons are observed above 8 ppm in the case of the parent clusters **1**, **3**, and **5** and the solvent-coordinated zwitterions[7] and at ca. 4.4 ppm for the η^2-imine-bridged clusters,[11,38] whereas the corresponding resonances of **1b** and **5b** are present around 5.1 ppm. In addition, IR spectra of the products **1b**−**5b** possess a weak ν(CO) band at 1700 cm^{-1}. According to the crystal structure of **2b**, which is representative for all products **1b**−**5b**, this ν(CO) band belongs to a CO ligand forming an Os−C(O)−N−Os bridge. To our knowledge such a bridge has never been observed for any other triosmium cluster, although it has been reported for the dinuclear compounds $Ru_2(CO)_6$(azadiene) and $Ru_2(CO)_6$(azaallyl)[48] and for isostructural diiron derivatives of the latter complex.[49] These binuclear complexes exhibit a similar low-frequency IR band (1682−1727 cm^{-1}) due to the bridging carbonyl ligand.

The bridging character of the imine group in **1b**−**5b** is reflected in the low value for the chemical shift of the imine proton (vide supra) and in the absence of an MLCT band in the visible region. According to the crystal structure of **2b**, the originally pendant NMe_2 group is coordinated to the $Os(CO)_2$(α-diimine) moiety in an equatorial position. The same will hold for the NMe_2 groups of **1b** and **5b** and for the 2-pyridyl groups of **3b** and **4b**. This conclusion agrees with the observation of two methyl resonances in the ^{1}H NMR spectra for the NMe_2 groups of **1b**, **2b**, and **5b**, which are 1.1 ppm apart, and also with the chemical shifts observed for the H1′−H4′ protons of the 2-pyridyl group in **4b**. In particular, the chemical shift of the *ortho*-proton H4′ (at 9.04 ppm in **4b** vs 8.56 ppm in **4**) points to the coordination of the 2-pyridyl group to the metal center. Finally, the increased splitting of the resonances of the CH_2 groups that link the NMe_2 and 2-pyridyl groups to the imine nitrogen clearly reflects the more pronounced asymmetry in the alkyl chain due to the coordination of the pendant group.

The Os−C(O)−N−Os bridge has a large influence on the bond distances within the Os cluster. This can best be seen from a comparison of the crystal structure of **2b** with those of $Os_3(CO)_{10}(\kappa^2N,N'$-*i*-Pr-DAB) (**7**) and in particular of the imine-bridged cluster $Os_3(CO)_{10}(\kappa^2N,N',\mu_2$-N′,$\eta^2$-N′═C-cPr−DAB)[38] **(8)**. The average Os−Os bond distance of **2b** (2.91 Å) compares well with that of the latter cluster (2.93 Å). However, due to the unusual Os−C(O)−N−Os bridge, the nonbonded Os1···Os2 distance of 3.91 Å in **2b** is even larger than that in the η^2-N′═C-bridged cPr−DAB cluster (3.59 Å). Similarly, the Os−C$^{(imine)}$ distance Os1−C6 of **2b** (2.22 Å) is significantly longer than that in the latter compound (2.14 Å), although this may be partly due to the steric hindrance between the $Os(CO)_3$ moiety and the CH_3 group bonded to C6. The formation of the imine bridge also causes a lengthening of the C═N′ bond. While this distance is 1.30 Å in the cluster **7**, it increases to 1.45 Å in cluster **8** and even to 1.50 Å in **2b**. The axial Os2−N1 distance in **2b** (2.11 Å) is comparable to those in the clusters **7** (2.11 Å) and **8** (2.12 Å). The Os2−N2 (2.20 Å) and Os2−N3 (2.27 Å) distances are, however, rather long. For the Os2−N2 distance this may be due to the Os−C(O)−N−Os bridge (with a strong C16−N2 bond of 1.51 Å). On the other hand, the long equatorial Os2−N3 distance indicates that the NMe_2 group is only weakly bound to the cluster. This is most likely caused by the restraints imposed by the short $(CH_2)_2$ chain, which prevents an optimal interaction of N3 with the metal. It is therefore not surprising that the product **2b** easily regenerates the parent cluster **2** in acetonitrile.

Mechanistic Aspects. The clusters **1**−**6**, all containing a potentially terdentate R−PyCa or R−AcPy ligand, were prepared in order to obtain zwitterions that are internally stabilized by the pendant Lewis base. In this way, zwitterions may be formed in any solvent, not only in coordinating ones such as acetonitrile. This permits characterization of such a zwitterion with time-resolved microwave conductivity (TRMC) and the choice of the most suitable solvent for the activation of small molecules such as olefins by the zwitterion.[50] Indeed, the internally stabilized zwitterion **6a′** ($\tau = 5$ s in 2-chlorobutane) could be detected by TRMC even at room temperature.[19] For the clusters **1**−**5** such zwitterions (**2a′** and **4a′**) were detected as unstable species upon irradiation of **2** and **4** at low temperature in 2-chloro-

(40) van Eldik, R.; Merbach, A. E. *Comments Inorg. Chem.* **1992**, *12*, 341.
(41) Skibsted, L. H.; Weber, W.; van Eldik, R.; Kelm, H.; Ford, P. C. *Inorg. Chem.* **1983**, *22*, 541.
(42) van Eldik, R.; Asano, T.; le Noble, W. J. *Chem. Rev.* **1989**, *89*, 549.
(43) Wieland, S.; van Eldik, R. *Coord. Chem. Rev.* **1990**, *97*, 155.
(44) Schneider, K. J.; van Eldik, R. *Organometallics* **1990**, *9*, 1235.
(45) Wieland, S.; Bal Reddy, K.; van Eldik, R. *Organometallics* **1990**, *9*, 1802.
(46) Fu, W. F.; van Eldik, R. *Inorg. Chim. Acta* **1996**, *251*, 341.
(47) Fu, W. F.; van Eldik, R. *Organometallics* **1997**, *16*, 572.
(48) Beers, O. C. P.; Delis, J. G. P.; Mul, W. P.; Vrieze, K.; Elsevier, C. J.; Smeets, W. J. J.; Spek, A. L. *Inorg. Chem.* **1993**, *32*, 3640.
(49) Mirkin, C. A.; Lu, K.-L.; Snead, T. E.; Young, B. A.; Geoffroy, G. L.; Rheingold, A. L.; Haggerty, B. S. *J. Am. Chem. Soc.* **1991**, *113*, 3800.
(50) Bakker, M. J.; Hartl, F. Unpublished results.

butane. At room temperature these clusters afford instead the novel Os−C(O)−N−Os-bridged photoproducts **1b**−**5b**.

The reaction pathways leading to the formation of **1b**−**5b** are presented in Scheme 1. In pyridine and acetonitrile light-induced homolysis of an Os−Os bond, coordination of a solvent molecule, and intramolecular electron transfer (these processes are probably concerted[7]) result in the formation of the zwitterions **1a.S**−**5a.S**. With the exception of **4a.S**, these zwitterions transform into the final products (**1b**−**3b**, **5b**). The zwitterion **4a.S** regenerates the parent cluster **4**. This behavior of **1a.S**−**3a.S** and **5a.S** is noteworthy since it points to replacement of a solvent molecule (i.e., acetonitrile) by the NMe_2 or 2-pyridyl sidearm of the α-diimine ligand to give **1a′**−**3a′** and **5a′**. This conformational change induces attack of the imine group bonded to the Os^+ center at the $Os(CO)_4^-$ moiety of the zwitterion to give **1b**−**3b** and **4b**. Although the photoreactions in acetonitrile do not produce the internally stabilized zwitterions **1a′**−**3a′** and **5a′** as detectable intermediates, irradiation of **2** and **4** in 2-chlorobutane at low temperature does afford such internally stabilized zwitterions **2a′** and **4a′**, which react further to give **2b** and **4b**, respectively. On the basis of this observation it is proposed that all products **1b**−**5b** are formed via the internally stabilized zwitterions **1a′**−**5a′** independent of the solvent used (Scheme 1). In noncoordinating solvents **1a′**−**5a′** are formed via the biradical initially produced on Os−Os bond homolysis from the reactive MLCT/$\sigma\pi^*$ excited state(s).[10] In addition, the transient photoproducts **2′** and **5′** are observed in 2-chlorobutane at low temperatures (183−203 K). Their two highest frequency ν(CO) bands identify them as structural analogues of an coordinatively unsaturated intermediate (see Figure 4c) previously observed in the formation of the isomers $(CO)_3Os-Os(CO)_4-Os(CO)_3(\kappa^2N,N',\mu_2\text{-}N',\eta^2\text{-}N'{=}C-R-PyCa)$ (see Figure 4b)[11] as the primary product of a radical coupling reaction between the $Os(CO)_4^{\bullet}$ and α-diimine$^{\bullet-}$ parts of the biradical transients. Due to their low yield, it could not be firmly established whether **2′** and **5′** only regenerate the starting cluster on heating or form parallelly also **2b** and **5b**, respectively. Both reactions are known to occur[11] for the structurally related intermediates depicted in Figure 4c, and **2′** and **5′** are assumed to play a similar role in the overall reaction mechanism (Scheme 1).

The methyl group at the imine carbon atom of the R−AcPy ligand hampers the formation of the Os−C(O)−N−Os-bridged product and destabilizes it. Thus, **6a′** does not provide such a product,[19] and the same holds for the zwitterion **4a.S** formed in acetonitrile or pyridine. In the case of **2** and **4** the formation of **2b** and **4b** out of the internally stabilized zwitterions **2a′** and **4a′** is sufficiently slow to allow detection of the latter species as intermediates at low temperature. For the R−PyCa clusters **1**, **3**, and **5** the formation of **1b**, **3b**, and **5b** is so rapid that no intermediates **1a′**, **3a′**, and **5a′** could be observed. Furthermore, **2b** and **4b** are apparently so destabilized by the steric hindrance of the methyl group on the imine carbon that they regenerate ultimately their parent cluster when formed in acetonitrile or toluene, respectively.

Apart from the steric demands of the methyl group, also the flexibility of the carbon chain connecting the Lewis base and the imine nitrogen influences the reaction. Thus, the zwitterion **2a′**, having two carbon atoms in the chain, is less stable than **6a′** and **4a′**, both having three carbon atoms. There is even a difference in stability between the latter two zwitterions, since **6a′** has a flexible chain of three sp^3 carbon atoms, whereas in the case of **4a′** one carbon atom is sp^2 hybridized, belonging to the 2-pyridyl group. Owing to this difference in flexibility, **6a′** is more stable than **4a′** and does not convert into the Os−C(O)−N−Os-bridged species **6b**.

The above effects are also reflected in the quantum yields of the photoreaction (Table 4). In pyridine and acetonitrile the Os−C(O)−N−Os-bridged isomers **1b**−**3b** and **5b** are formed via the solvent-coordinated zwitterions **1a.S**−**3a.S** and **5a.S**, and the quantum yields are mainly determined by the efficiency of the zwitterion formation. This is evident from the close correspondence between the quantum yields of solvent-stabilized zwitterion formation for triosmium clusters with ordinary bidentate α-diimine ligands in pyridine (ca. 0.20−0.34) [7] and those for the formation of **1b**, **2b**, and **5b** in acetonitrile. The latter quantum yields are much higher in acetonitrile than in toluene, where internally stabilized zwitterionic intermediates are involved (Table 5). This difference reflects the lower efficiency of the formation of the internally stabilized zwitterions compared to the facile formation of their solvent-stabilized counterparts. First of all, acetonitrile easily cleaves a weakened metal−metal bond of the parent cluster in its MLCT/$\sigma\pi^*$ excited state,[10] producing first a long-lived solvent-stabilized zwitterion. In contrast, toluene hardly affects the reactivity in the MLCT/$\sigma\pi^*$ state, and the parent clusters therefore primarily produce short-lived biradicals in this solvent instead. Because of the short lifetime, the biradicals preferably undergo the reverse Os−Os bond closure before the pendant sidearm can coordinate to the metal and induce the conversion into the internally stabilized zwitterions as the intermediate to form the ultimate Os−C(O)−N−Os-bridged product (see Scheme 1). In addition, part of the biradicals also undergo a radical coupling reaction producing the intermediates **2′** and **5′**. The fate of **2′** and **5′** (recovery of **2** and **5** and/or formation of **2b** and **5b**) is not fully clarified. However, this minor pathway cannot contribute significantly to the net product formation. In the case of **1** and **5**, the quantum yield is higher in THF than in toluene, since the biradicals are formed more efficiently in the former solvent and their lifetimes are also longer. The influence of the solvent is also apparent from the activation energies E_a derived from the temperature dependence of the quantum yields in THF and toluene. For cluster **5**, E_a appeared to be much lower in THF (190 ± 10 cm^{-1}) than in toluene (510 ± 15 cm^{-1}). The above behavior does not apply to **2**, since for this cluster the quantum yield in toluene hardly differs from that in THF. The rather low quantum yield in THF is probably caused in this case by the unfavorable coordination of the shorter $-(CH_2)_2-NMe_2$ sidearm which has to substitute THF in the biradical transient. This is also apparent from

the instability of both **2a′** (compared to **6a′** and **4a′**) and **2b** (in acetonitrile).

The nonlinear relationship between $\ln(\Phi_5)$ and $1/T$ in THF points to the presence of two temperature-dependent reaction pathways of **5** in this solvent. This is quite understandable in view of the fact that THF acts as a much stronger Lewis base at low temperatures. This phenomenon has also been reported for the clusters $Os_3(CO)_{10}(\kappa^2 N,N'$-α-diimine)[7,9] and for the dinuclear complexes $Mn_2(CO)_8$(α-diimine).[6] In the latter case, the dimers $Mn_2(CO)_{10}$ and $Mn_2(CO)_6$(α-diimine)$_2$ were produced at ambient temperature, whereas below 200 K the charge-transfer products $Mn(CO)_5^-$ and Mn^+(THF)$(CO)_3$(α-diimine) were observed. Thus, in the case of **5**, THF only induces the formation of relatively long-lived biradicals at room temperature, while at sufficiently low temperatures THF-coordinated zwitterions **5a.THF** are produced (see Scheme 1).

Finally, the very small positive volume of activation ($\Delta V^{\ddagger} = +2.6 \pm 0.6$ cm^3 mol^{-1}) for the formation of **5b** from **5** in toluene shows that the increase in volume due to the Os−Os bond opening in the rate-determining step(s) is less than for the formation of the solvent-coordinated zwitterion $(CO)_4Os^-Os(CO)_4Os^+$(pyridine)$(CO)_2$(nPr−AcPy) in pyridine ($+7.0 \pm 0.5$ cm^3 mol^{-1}),[7] eventhough **5b** is also formed via a zwitterion. In the case of $Os_3(CO)_{10}$(nPr−AcPy), the positive effect of the Os−Os bond opening on $\Delta V^{\ddagger}$ is partly offset by the coordination of a solvent molecule. For **5b**, this effect is replaced by the coordination of the pendant NMe_2 group. Such coordination greatly reduces the volume occupied by the sidearm, and hence the positive volume effect of the Os−Os bond cleavage is nearly canceled for **5b**.

Conclusions

In the triosmium clusters **1**−**5**, the Me_2N− or 2-pyridyl functions of the pendant sidearm R at the imine nitrogen of the *N,N′*-chelated R−PyCa and R−AcPy ligands (L) play a crucial role in the reaction pathway after the light-induced cleavage of an $(CO)_4Os$−Os$(CO)2$(L) bond. (i) Differently from the previously studied photochemistry of corresponding $Os_3(CO)_{10}$(L) clusters with virtually bidentate R−PyCa and R−Acpy (R = alkyl) ligands, intramolecularly stabilized zwitterions can be produced in weakly or noncoordinating solvents upon coordination of the pendant Lewis base to the Os$(CO)_2$(L) moiety of the open triosmium core. The stability of the latter zwitterions can be tuned by varying flexibility of the carbon chain of the R arm. Increasing steric hindrance on the imine carbon atom (R−AcPy vs R−PyCa) hampers the subsequent formation of the ultimate Os−C(O)−N−Os-bridged products **1b**−**5b** or may even prevent it completely[19] in the case of **6**, where both stabilizing factors are most effective. (ii) The photoisomers **1b**−**5b** also owe their relative stability to the coordination of the pendant Lewis base, which prevents a transfer of a CO ligand from the adjacent $Os(CO)_4$ moiety to the $Os(CO)_2$(L) site in order to compensate for an unbalance in metal coordination. The latter transformation via two CO-bridged (Os−C(O)−N) intermediates was indeed observed[11] for corresponding $Os_3(CO)_{10}$(L) clusters with virtually bidentate R−PyCa and R−DAB ligands (R = alkyl).

Acknowledgment. We thank Prof. R. van Eldik and his group for the opportunity to perform the pressure-dependent quantum yield measurements at Erlangen-Nürnberg University and for helpful discussions on this subject, and Dr. W.-F. Fu for his elaborate assistance with the experiments.

Supporting Information Available: Complete tables of crystallographic data, positional parameters, anisotropic thermal parameters, bond lengths, and bond angles of the photoproduct **2b**. This material is available free of charge via the Internet at http://pubs.acs.org.

OM990366O